Catena 90 (2012) 26–38

Contents lists available at SciVerse ScienceDirect

Catena

journal homepage: www.elsevier.com/locate/catena

Holocenic proxies of sedimentary organic matter and the evolution of Lake Arari-Amazon Region

C.B. Smith [a], M.C.L. Cohen [a,b,*], L.C.R. Pessenda [c], M.C. França [a], J.T.F. Guimarães [a]

[a] Post-Graduate Program of Geology and Geochemistry, Laboratory of Coastal Dynamics, Federal University of Pará, Avda Perimentral 2651, Terra Firme, CEP: 66077-530, Belém (PA), Brazil
[b] Faculty of Oceanography, Federal University of Pará, Rua Augusto Corrêa 1, Guama, CEP: 66075-110, Belém (PA), Brazil
[c] University of São Paulo, 14C Laboratory, Avenida Centenário 303, 13416000 Piracicaba, SP, Brazil

ARTICLE INFO

Article history:
Received 14 January 2011
Received in revised form 31 August 2011
Accepted 18 October 2011

Keywords:
Amazon River
C and N isotopes
Marajó Island
Palynology
Relative sea-level
Wetland development

ABSTRACT

Four sediment cores were sampled from Lake Arari, located on Marajó Island at the mouth of the Amazon River. The island's vegetation cover is composed mainly of Amazon coastal forest, herbaceous and varzea vegetation. The integration of data on sedimentary structures, pollen, carbon and nitrogen isotope records, C/N ratios and radiocarbon ages allowed the identification of changes in vegetation and the sources of organic matter accumulated in the lake during the Holocene. The data indicate a relatively high flow energy, marine water influence and the presence of mangroves during the lagoon phase between 8990 and 8690 cal yr B.P. and 2310–2230 cal yr B.P. Between 2310 and 2230 cal yr B.P. and ~1000 cal yr B.P., the flow energy decreased and the mangroves were replaced by herbaceous vegetation following the decline in marine influence, likely due to the increase in freshwater river discharge. During the last 1000 years, Lake Arari was established in association with the expansion of herbaceous vegetation and the dominance of freshwater algae.

1. Introduction

Palaeoenvironmental research in the northern Brazilian littoral suggests continuous vegetation shifts due to climatic and sea-level fluctuations, and is characterized mostly by mangrove vegetation dynamics (Behling et al., 2001a; Cohen et al., 2008, 2009; Lara and Cohen, 2009; Vedel et al., 2006). Such forests are considered to be indicators of coastal changes (e.g. Blasco et al., 1996), since the evolution of this ecosystem is controlled by land–ocean interactions (Woodroffe, 1982). Also, Krauss et al. (2008) described the effects that multiple ecological factors may have on mangrove development, and concluded that salinity, light, nutrients, flooding, temperature, and sea-level changes are important drivers of mangrove establishment on a global scale.

Regarding the eastern littoral of the mouth of the Amazon River, pollen studies show mangrove establishment between 7500 and 5100 cal yr BP (Behling and Costa, 2001; Behling et al., 2001a; Cohen et al., 2005a,b, 2009; Vedel et al., 2006), reflecting the post-glacial sea level rise that invaded the coast, which is embayed by rather shallow and broad valleys (Cohen et al., 2005a). The western littoral of the river has seen mangroves develop during the last 2000 cal yr B.P., with alternations between mangrove and varzea forest that reflect marine and freshwater influence (Guimarães et al., 2010).

Mangrove vegetation on Marajó Island at the mouth of the Amazon River is currently restricted to the eastern side, and has developed continuously since 2700 cal yr B.P. (Behling et al., 2004). According to pollen records from hinterland (Lake Arari), the area covered by mangrove vegetation was largest between 750 and 500 cal yr B.P. (Cohen et al., 2008).

Toledo and Bush (2007) recorded, ~10 km away from the Amazon River, a declining proportion of *Rhizophora* pollen after ca. 7000 cal. yr B.P., suggesting a lessening of marine influence and, from 5000 cal yr B.P., the replacement of dense forest elements by open flooded savanna. This study suggests a reduction in Amazon River discharge due to a dry period in the Andes, when precipitation levels markedly decreased between 8000 and 5000 cal yr B.P.

In order to complement pollen analyses, analyses of stable carbon and nitrogen isotopes ($\delta^{13}C$, $\delta^{15}N$) and the C/N ratio of organic matter preserved in soils and sediments have been used in palaeoenvironmental studies in other regions of Brazil (Desjardins et al., 1996; Freitas et al., 2001; Gouveia et al., 1997, 1999; Pessenda et al., 1996, 1998a,b,c, 2001a). On Marajó island, the integration of facies analysis, $\delta^{13}C$, $\delta^{15}N$, C/N ratios and radiocarbon dating demonstrated successive palaeoenvironmental changes as consequences of relative sea-level fluctuations during the late Pleistocene (Miranda et al., 2009).

The work presented here includes a modern phytoplanktonic characterization, $\delta^{13}C$, $\delta^{15}N$, C/N analyses and radiocarbon dating of organic matter preserved during the Holocene in four sediment

* Corresponding author at: Post-Graduate Program of Geology and Geochemistry, Laboratory of Coastal Dynamics, Federal University of Pará, Avda Perimentral 2651, Terra Firme, CEP: 66077-530, Belém (PA), Brazil. Tel.: +55 91 3274 3069.
E-mail address: mcohen@ufpa.br (M.C.L. Cohen).

0341-8162/$ – see front matter © 2011 Elsevier B.V. All rights reserved.
doi:10.1016/j.catena.2011.10.002

cores sampled from Lake Arari, (Marajó Island in Northern Brazil), in order to significantly complement and improve the pollen and facies interpretations used in paleoenvironment reconstruction studies.

2. Study area

Lake Arari (0°35′0.34″S/49°08′3.70″W to 00°45′21.77″S/49° 09′ 20.76″W) is located on the central-eastern portion of Marajó Island, which is dominated by Quaternary deposits derived from the fluvial/estuarine environment (currently disabled) and characterized by a series of dendritic and anastomosing channels (Cohen et al., 2008).

This lake is a N–S elongated feature with 2–4 m depth distributed over about 100 km^2, and its drainage basin area is estimated to be at least 2000 km^2. Located ~70 km from the modern coastline, it is connected to the Atlantic Ocean by the Tartarugas channel. The southern part of the lake forms the headwaters of the Arari River, which drains to the southeast into Marajó Bay.

The waters of Lake Arari are rich in suspended material from the erosion of sedimentary rocks found along its drainage basin, with values of total dissolved solids, dissolved oxygen and salinity from 7 to 12 mg/L, 2 to 5 mg/L and 0‰, respectively.

The climate is tropical warm and humid, with a mean annual temperature of 27 °C and mean annual precipitation of approximately 2680 mm, concentrated between January and June (IDESP, 1974). During the dry season (July to December) rainfall is the lake's main water source and its area is reduced by ~80%. Macrophytic vegetation, which covers about 20% of the lake's area, is not found during this period.

Vegetation around the lake consists of natural open areas dominated by Cyperaceae and Poaceae that colonize mainly the eastern side of the island of Marajó, while the Varzea vegetation (composed of wetland trees such as *Euterpe oleracea* (açai) and *Hevea guianensis* (seringueira) and "Terra Firme" vegetation (composed of terrestrial trees such as *Cedrela odorata* (cedar), *Hymenaea courbaril* (Jatoba) and *Manilkara huberi* (Maçaranduba)) occur on the western side (Cohen et al., 2008). Narrow and elongated belts of dense ombrophilous forest are also present along riverbanks (Rossetti et al., 2008b). The coexistence of periodically wet and permanently dry open areas covered with herbaceous vegetation, as well as "Terra Firme" vegetation on Marajó Island has been explained by vegetational succession (Whitmore, 2009), where herbaceous stands have been progressively replaced by "Terra Firme" vegetation (Rossetti et al., 2010) following vegetation adaptation to a slightly positive topography.

3. Materials and methods

3.1. Sampling sites and sample processing

Fieldwork was undertaken during the transition between the rainy and the dry season in 2007. Leaves of the most representative macrophytes of Lake Arari were sampled for isotopic determination (Table 1). Four sites were selected on the lake for phytoplankton and water sampling (Fig. 1 and Table 2). Water depth, Secchi disk visibility, conductivity and pH (multi-parameter probe Hanna HI9828) were measured *in situ*. Four sediment cores (LA-A, LA-B, LA-C and LA-D) were taken from the bottom of the lake under a water depth of 1.5–2.0 m. The cores were collected using a "Russian" sampler. The top five centimeters from each core were lost during sampling. The samples were submitted to X-ray analysis to identify internal structures, their color was defined using a Munsell soil chart and their particle size distribution was determined by a laser particle analyzer (SHIMADZU SALD 3101) and the graphics were analyzed with the SysGran Program (Camargo, 1999).

These properties of sediment can reveal information about the environment of deposition. This is especially true of sedimentary structures and grain size, features in sediment that develop during specific fluid flow regimes. As flow energy is often indicative of specific transport processes, and, therefore, the associated environments where these processes can occur, the presence of sedimentary structures helps to interpret the environment of sediment deposition (e.g. Boggs, 2012).

Table 1
List of macrophytes of Lake Arari and their $\delta^{13}C$ value.

Division or Family	Espécie	^{13}C (PDB)
Araceae	*Pistia stratioides*	−26.64
Convolvulaceae	*Ipomoea asarifolia*	−28.22
Leguminosae/ Mimosoideae	*Neptunia prostata*	−30.01
Leguminosae/ Papilionoideae	*Aeschynomene sensitive*	−29.11
Lentibulariaceae	*Utricularia* sp.	−30.40
Magnoliophyta	unidentified	−28.24
Magnoliophyta	unidentified	−29.60
Menyanthaceae	*Nymphoides indica*	−25.30
Onagraceae	unidentified	−29.49
Poaceae	unidentified	−28.75
Poaceae	*Echinochloa polystachya*	−10.68
Poaceae	*Hymenachne amplexicaulis*	−29.24
Poaceae	*Leersia hexandra*	−27.84
Poaceae	*Luziola Spruceana*	−28.06
Poaceae	*Oryza rufipogon*	−29.04
Poaceae	*Paspalum repens*	−10.99
Pteridophyta	*Ceratopteris pterioides*	−27.72
Pteridophyta	*Marsilea quadrifolia*	−27.07
Pteridophyta	*Salvinia auriculata*	−28.24
Pontederiaceae	*Eichhornia crassipes*	−28.80
Rubiaceae	Borreria sp.	−29.34
Rubiaceae	Borreria sp.	−30.17

3.2. Pollen analysis

For pollen analyses, 1 cm^3 samples were taken at 2.5 cm intervals along the cores. Sample preparation followed standard pollen analytical techniques including acetolysis (Faegri and Iversen, 1989). Most pollen types were identified based on published morphological descriptions (Colinvaux et al., 1999; Herrera and Urrego, 1996; Roubik and Moreno, 1991) and the reference pollen collection of the Coastal Dynamics Laboratory of the Federal University of Pará. A minimum of 300 pollen grains were counted for each sample, except at certain depths where only 100–200 grains were counted. Microfossils consisting of spores, algae and some fungi were also counted, but not included in the sum. Software package TILIA was used for calculations, CONNIS for the cluster analysis of pollen taxa and TILIAGRAPH for plotting the pollen diagrams (Grimm, 1987).

3.3. Radiocarbon analysis

Eight subsamples were taken for Accelerator Mass Spectrometer (AMS) radiocarbon dating, performed at the Leibniz Laboratory of Isotopic Research at Christian Albrechts University in Kiel (Germany), and the Center for Applied Isotope Studies at the University of Georgia (USA). Radiocarbon ages are presented in conventional yr B.P. and in cal yr B.P. ($\pm 2\ \sigma$), according to Reimer et al. (2004).

3.4. Isotopic and chemical analyses

Forty five samples (1 cm^3) were collected at 5 cm intervals along the sediment cores. Samples of leaves, roots, etc., were separated and treated with 4% HCl to eliminate carbonates, washed with distilled water until the pH reached 6, dried at 50 °C and homogenized. These samples were used for total organic carbon and nitrogen analyses, carried out at the Stable Isotope Laboratory of the Center for Nuclear Energy in Agriculture (CENA/USP). The results are expressed in percentage of dry weight, with analytical precision of 0.09 and 0.07%, respectively. The ^{13}C and ^{15}N results are expressed as $\delta^{13}C$

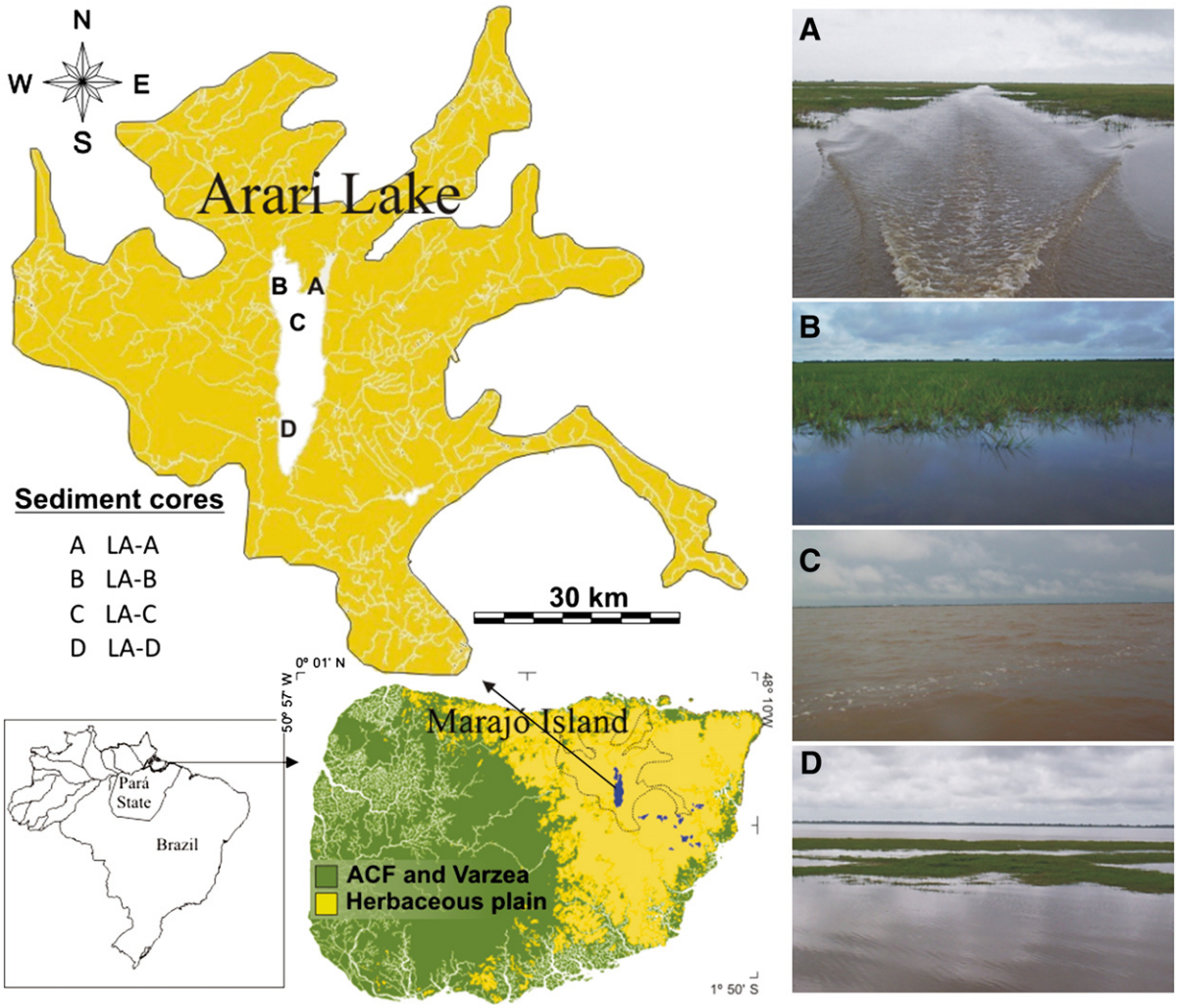

Fig. 1. Study site with vegetation units and photographs of the sampling sites.

and $\delta^{15}N$ with respect to the PDB standard and atmospheric air, respectively, using the following conventional notations:

$$\delta^{13}C_{Sample} = \frac{R_{S1} - R_{PDB}}{R_{PDB}} \times 1000$$

$$\delta^{15}N_{Sample} = \frac{R_{S2} - R_{Air}}{R_{Air}} \times 1000$$

where R_{S1} and R_{S2} are, respectively, the $^{13}C/^{12}C$ and $^{15}N/^{14}N$ ratios in the sample, RPDB the $^{13}C/^{12}C$ ratio for the international standard (PDB) and RAir the $^{15}N/^{14}N$ ratio for atmospheric air. The results were expressed in delta per mil (δ ‰) notation, with analytical precision better than 0.2‰ (Pessenda et al., 2004a).

Table 2
Sampling coordinates.

Sampling points	Collected material	Geographic coordinates
LA-A	63 cm of sediment	S 00° 35′ 52.1″, W 49° 08′ 35.2″
LA-B	82 cm of sediment	S 00° 35′ 54.0″, W 49° 09′ 49.9″
LA-C	50 cm of sediment	S 00° 39′ 39.1″, W 49° 09′ 20″
LA-D	80 cm of sediment	S 00° 43′ 40.9″, W 49° 10′ 00.4″

3.5. Phytoplankton

Phytoplankton samples were fixed in formalin and algal counts (cells, colonies and filaments) were evaluated under an Olympus CH 30 microscope. Prepared samples were transferred to a settling chamber (2.5 or 5 ml capacity), and at least 100 individuals of the most numerous algae were counted per sample. The classification system used for the Chlorophyta, Cyanophyta and Bacillariophyta were Bourrelly (1972), Desikachary (1959) and Round et al. (1990), respectively. The identifications were based on Bicudo (1970); Bourrelly (1972); Cleve-Euler (1953); Desikachary (1959); Förster (1974); Hino and Tundisi (1984); Hustedt (1930); Komárek and Fott (1983); Peragallo and Peragallo (1908).

4. Results

4.1. Physical, chemical and biological characteristics of Lake Arari

Secchi depth is between 35 and 160 cm, salinity is null and the pH ranges between 6 and 8.2. Total dissolved solids and oxygen levels were found to lie between 7 and 12 and 3.3 and 5.5 mg/l, respectively. The mean water temperature was about 27 °C.

Forty one phytoplankton species were identified (Table 3). The Chlorophyta division is represented by 36 species, while the Bacillariophyta and Cyanohyta are represented by 4 and 1 species, respectively, which are typical of freshwater (Cooper, 1999; Parra and Bicudo,

Table 3
List of phytoplankton of Lake Arari.

Chlorophyta	Cyanophyta	Bacillariophyta
Spirogyra sp	*Oscillatoria sp*	*Polymyxus coronalis*
Micrasterias torrely		*Melosira sp*
Desmidium laticeps		*Corethron sp*
Staurastrum sexangulari		*Aulacoseira granulata*
Staurastrum leptacanthum		
Staurosdesmus cornutus		
Staurastrum nudibrachiatum		
Micrasterias laticeps var. minor		
Xanthidium canadense		
Pleurotaenium cylindricum		
Closterium sp		
Spondylosium pulchrum		
Zignema sp		
Oedogonium		
Xanthidium trilodum		
Onychonema laeve		
Staurodesmus megacanthus		
Micrasterias mahabuleshwarensis		
Eudorina elegans		
Gonatozygon kinahani		
Micrasterias radiosa		
Volvox aureus		
Desmidium baileyi		
Spondylosium panduriforme		
Eunotia zygodon		
Closterium ehrenbergii		
Staurastrum minnesotense		
Closterium kuetzingii		
Spirogyra ellipsospora		
Hyalotheca disilliens		
Staurastrum rotula		
Bambusina brebissonii		
Ankistrodesmus sp		
Closterium pronum		
Cosmarium denticulatum		
Spondylosium moniliforme		

1995). The exception was *Polymyxus coronalis* that can also be found in estuarine waters (Monteiro et al., 2009; Navarro and Peribonio, 1993; Paiva et al., 2006), however its abundance was low (<1%).

4.2. Textural and pollen description of the sediment cores

The sediments studied include mostly dark gray and light brown, either muddy or sandy silt that is locally interbedded with fine-grained sand (Fig. 2). These deposits are massive, parallel laminated or heterolithic bedded (mostly wavy).

4.2.1. LA-A core

The base (Fig. 2, 63–45 cm; 3790–3710 cal yr B.P.–~2700 cal yr B.P) of the LA-A core displays a transition of light gray muddy silt with discontinuous lenses of fine-grained sand to a muddy silt with thin parallel lamination of fine-grained sand. The pollen assemblage indicates herbaceous vegetation with mangrove species such as *Rhizophora* and *Avicennia* (Fig. 2). The LA-A core is the most exposed to marine influence since it is close to the Tartarugas Channel, which is connected to the sea.

The 45–30 cm interval (~2700–~2000 cal yr B.P.) exhibits greenish gray sandy silt layers interbedded with fine-grained sand forming wavy structures and filling the top of this section with light brown massive muddy silt. Pollen preservation was not observed in the 42.5–32.5 cm interval (Fig. 2). It may be caused by various external factors (sediment grain size, microbial attack, oxidation, mechanical forces, high temperature), as well as factors inherent to the pollen grains themselves (sporopollenine content, chemical and physical composition of the pollen wall) (e.g. Havinga, 1967). However, considering the 42.5–32.5 cm interval with sandy silt layers interbedded with fine-grained sand, the sediment grain size may be considered the main cause to the absence of pollen grains, because sandy sediments are not suitable to the pollen preservation.

The 30–20 cm interval (~2000–~1400 cal yr B.P.) is characterized by a thin parallel lamination of fine-grained sand in light brown muddy silt with the predominance of herbaceous pollen. The last 20 cm consists of dark gray massive sandy silt with herbaceous pollen.

4.2.2. LA-B

The LA-B core (Fig. 3) contains, between 82 and 72 cm (4530–4420 cal yr B.P.–~3800 cal yr B.P.), light gray muddy silt with thin parallel lamination of fine-grained sand accumulated with herbaceous and mangrove pollen (Fig. 3). The transition section between 72 and 65 cm (~3800–~3400 cal yr B.P.) is characterized by sandy silt with wave structures and the predominance of herbaceous pollen. The 65–40 cm interval (~3400–~1200 cal yr B.P.) displays a grain size gradient along muddy silt with thin parallel lamination of fine-grained sand and the presence of herbaceous pollen exclusively. This trend is maintained to the top of the core where the 20–0 cm section (~350 cal yr B.P.–present) exhibits massive muddy silt with only herbaceous pollen.

4.2.3. LA-C

The LA-C core (Fig. 4) contains, between 50 and 40 cm (8990–8690 cal yr B.P.–~7000 cal yr B.P.), light gray muddy silt with thin parallel lamination of fine-grained sand. The 40–0 cm interval (~7000 cal yr B.P.–present) exhibits a gradual transition, with parallel laminated muddy silt that grades upward into massive muddy silt. The low pollen amounts along this core did not allow for a suitable statistical analysis. It may be attributed to an eventual exposition to the atmospheric air that produces pollen oxidation (e.g. Keil et al., 1994).

4.2.4. LA-D

In contrast to the LA-A and LA-B cores, which were sampled closer to the Tartatuga Channel and relatively more influenced by marine waters, the LA-D core was sampled closer to the Arari River (Fig. 1). Its base (Fig. 5) (80–60 cm, 7330–7170 cal yr B.P.–~6700 cal yr B.P) is characterized by muddy silt with thin parallel laminations of fine-grained sand, while between 60 and 40 cm (~6700–~6200 cal yr B.P.) it displays wavy structures. Between 40 and 20 cm (6200–2270 cal yr B.P.), muddy silt occurs again with thin parallel laminations of fine-grained sand. This sequence revealed a predominance of mangrove pollen (Fig. 5). Over the last 20 cm, sand laminations in muddy silt with predominantly mangrove pollen gradually change to massive muddy silt with herbaceous pollen dominance.

4.3. Total organic carbon (TOC)

Figs. 2, 3, 4 and 5 show the amounts of total organic carbon (TOC) in the four sediment cores taken at Lake Arari. Throughout the LA-A core there is an increase in TOC from the bottom (0.25%) to the top (0.5%), with a slight reduction at 40 cm depth (0.26%). The LA-B core shows TOC contents around 0.2% from the bottom to 20 cm depth, and then an increase to 1.6% near the top. The 50–30 cm layer of the LA-C core shows values around 0.16%, and an increase to 0.45% at 10 cm depth. The TOC values for the LA-D core range between 0.2 and 0.3% from the sediment bottom to 20 cm depth, followed by an increase up to 0.6% near the surface.

4.4. $\delta^{13}C$ of macrophytes from Lake Arari

Among the 25 macrophytes analyzed for $\delta^{13}C$ (Table 1), only 2 species of Poaceae, *Paspalum repens* ($\delta^{13}C = -10.99‰$) and *Echinochloa polystachya* ($\delta^{13}C = -10.68‰$) are C_4 plants. These species and *Oryza rufipogon* ($\delta^{13}C = -29.04‰$), a C_3 grass, are the most representative

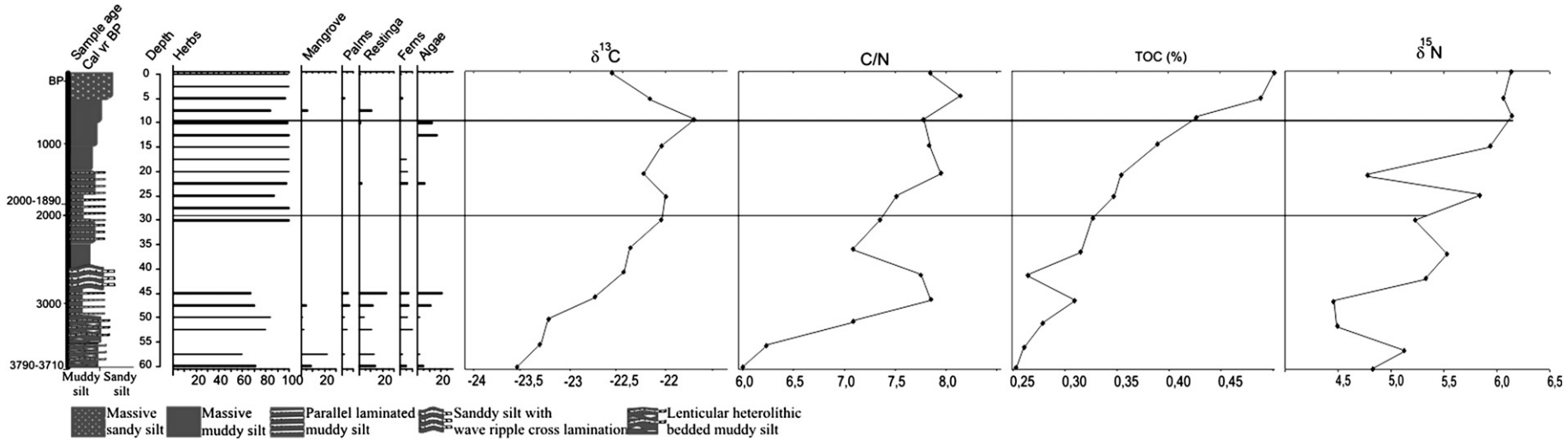

Fig. 2. Stratigraphy, pollen diagram and isotopic characteristics of core LA-A.

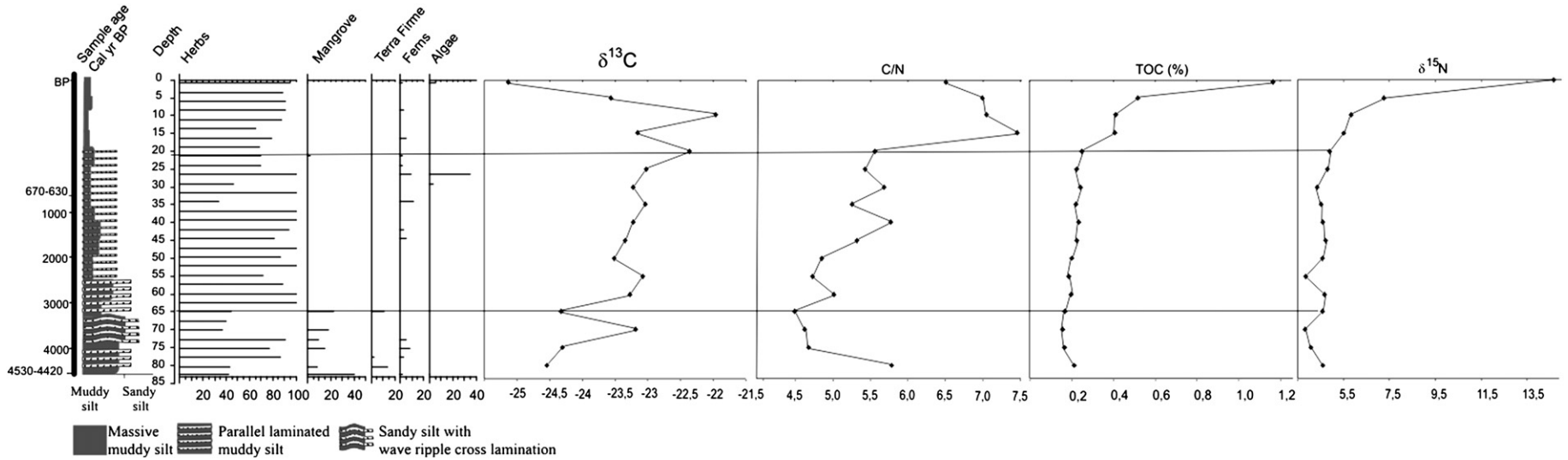

Fig. 3. Stratigraphy, pollen diagram and isotopic characteristics of core LA-B.

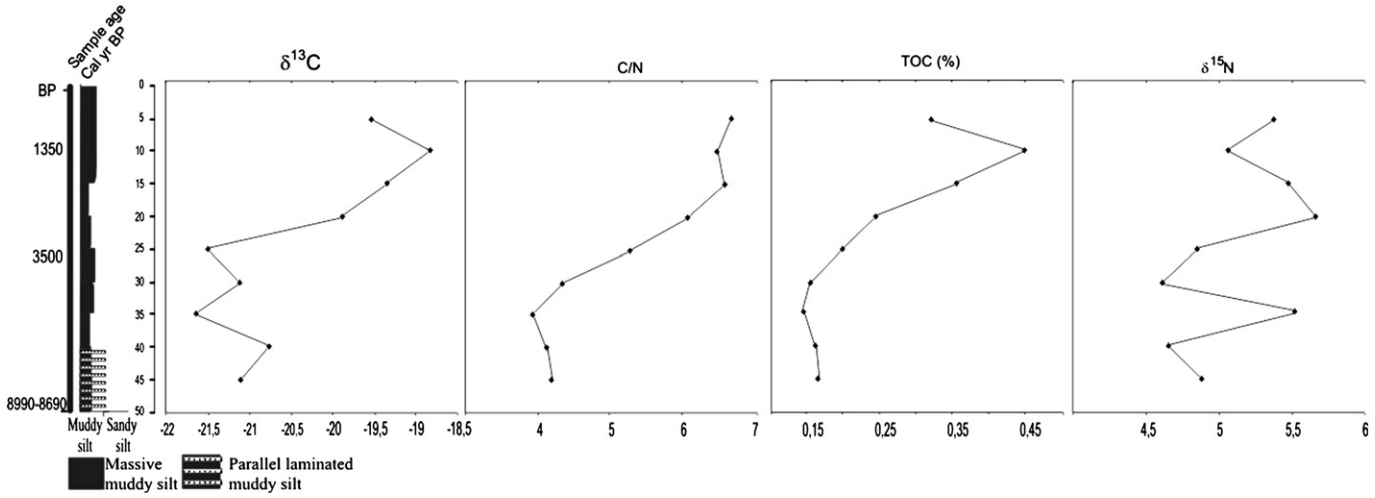

Fig. 4. Stratigraphy and isotopic characteristics of core LA-C.

aquatic plants of the lake. Lima (2008) analyzed the $\delta^{13}C$ of the most representative plant species around the lake and found that C_3 plants were dominant. The $\delta^{15}N$ values of C_3 macrophytes *Nymphoides aquatica*, *Utricularia foliosa* and *Utricularia purpurea* from the Everglades, Florida, USA were 3.03, 5.81 and 4.53‰, respectively (Troxler and Richards, 2009), while the C_4 macrophyte *Paspalum repens* gave a value of 4.1‰ (Fellerhoff et al., 2003). These genera occur on Lake Arari (Table 1), and their expansion during the lake phase may have contributed to the $\delta^{15}N$ values of the analyzed cores.

4.5. $\delta^{13}C$, $\delta^{15}N$ and C/N composition of sedimentary organic matter

The LA-A core (Fig. 2) shows a $\delta^{13}C$ enrichment trend, with values rising from −23.5‰ to −21.8‰ along the 60–10 cm interval. A depletion is observed over the last 10 cm, to −22.6‰. An enrichment in $\delta^{15}N$ was also observed with rising from 4.8‰ to 6.2‰, but with a depletion in the 50–45 cm interval (4.5‰) and at 20 cm depth (4.8‰). The C/N ratio varied from 6 to 8.1.

The $\delta^{13}C$ values for the LA-B core (Fig. 3) varied between −24‰ and −22‰ along the 80–10 cm interval to more depleted values (−25‰) near the top. For the 80–20 cm interval, $\delta^{15}N$ values varied from 3.8 to 4.9‰ with enrichment up to 14.6‰ near the top of the core. The C/N ratio varied between 4.5 and 7.5.

The $\delta^{13}C$ values for the LA-C core (Fig. 4) were stable around −21‰ between 45 and 25 cm, with an enrichment trend upward (−19‰). The $\delta^{15}N$ values varied between 4.5 and 5.5‰, and the C/N ratio from 4 to 6.5.

The $\delta^{13}C$ values of the LA-D core varied from −25.7 to −23.7‰, and the $\delta^{15}N$ values from 7.6 to 5.8‰. The C/N ratio varied from 6.3 to 8 in the 75–20 cm interval up to 9.6 near the top of the core.

5. Discussion

5.1. Organic matter source

According to Meyers and Lallier-Vergès (1999), the concentration of TOC is a fundamental parameter for describing the abundance of organic matter in sediments. Overall organic carbon contents of the sediments in this study are relatively low (0.2–0.5%) in relation to values obtained in other Amazonian lakes, such as Calado Lake (2–4% in fine detrital mud) (Behling et al., 2001b), Caracarana Lake (4–10% in clay) (Turcq et al., 2002), Carajas Serra Sul Lake (20–60% in clastic layers) (Sifeddine et al., 1994) and in the lakes of the Várzea do Lago Grande de Curuai (0.6–37%) (Moreira-Turcq et al., 2004). Low values for TOC in Amazonian sediment lakes are related to dry episodes (Moreira et al., 2009; Sifeddine et al., 1994) or a greater contribution of phytoplanktonic organic matter (Turcq et al., 2002). Despite the relatively low TOC values observed here, the carbon data follows the typical pattern of decreasing carbon content with depth (Figs. 2, 3, 4 and 5).

The $\delta^{13}C$ profiles obtained from the four cores collected in Lake Arari show variations at least during the last ~8900 cal yr B.P. Changes in carbon isotope signatures were observed along the cores with variations between −25.6 and −18.8‰, which is indicative of a predominance of C_3 plants (−25 to −23‰) and a mixture of C_3 and C_4 plants (−22 to −18‰) (Pessenda et al., 2001b, 2010) and/or freshwater/marine algae influence (−30‰ to −26‰ and −23‰ to −16‰, respectively, Schidlowski et al., 1983, Meyers, 1994) (Figs. 6 and 7). The $\delta^{13}C$ enrichment trend observed from the bottom to 10 cm depth of the LA-A core (−23.5‰ to −22‰, ~3750 to ~720 cal yrs B.P., Fig. 2), the LA-B core (−24.6‰ to −21.9‰, ~4470 to ~200 cal yrs B.P., Fig. 3), the LA-C core (−21‰ to −18.8‰, 8990–8690 to ~1350 cal yr B.P., Fig. 4) and the LA-D core (−25‰ to −24‰, 7330–7170 to ~2000 cal yrs B.P., Fig. 5) can be related to greater contributions of marine phytoplankton (−23‰ to −16‰) and/or C_4 plants (−17‰ to −9‰). The extent of $\delta^{13}C$ depletion in the upper layer (10 cm) is too large to be associated with greater influence of freshwater organic matter and/or C_3 plants. The pollen record for the four sediment cores (Figs. 2, 3, 4 and 5) suggests a mixture of brackish and freshwater, given the dominance of mangrove (brackish water vegetation) pollen between 7328–7168 and 2310–2230 cal yr B.P., followed by herbaceous (freshwater vegetation) pollen until present (Fig. 5).

The relationship between $\delta^{13}C$ and C/N values (Fig. 7) indicates a significant contribution of marine algae and the lesser influence of freshwater algae in relation to vascular plants, mainly in the LA-A, LA-B and LA-C cores during the period 8990–8690 to ~400 cal yr BP. The period 7330–7170 cal yr B.P. until present in the LA-D core indicates a mixture of marine and freshwater algae.

The results for nitrogen isotope content in sedimentary organic matter are shown in Figs. 2, 3, 4 and 5, and indicate a mixture of algae and aquatic plants represented by values between 4 and 7.5‰. Aquatic plants use dissolved inorganic nitrogen, which is isotopically enriched in ^{15}N by 7 to 10‰ relative to atmospheric N (0‰), thus terrestrial plants that use N_2 derived from the atmosphere have $\delta^{15}N$ values ranging from 0 to 2‰ (Meyers, 2003). Samples from shallow depths gave values between 6 and 14‰ and this indicates a trend to phytoplankton-derived organic matter, since the phytoplankton utilize the ^{15}N-rich nitrate and give values for $\delta^{15}N$ up to 18‰ (Sharp, 2007).

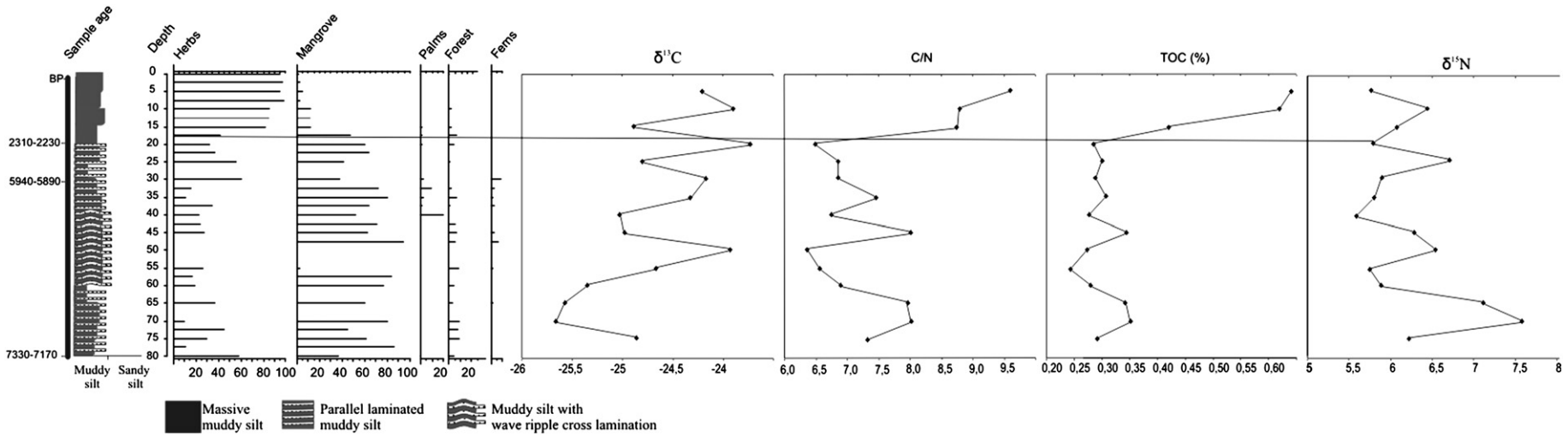

Fig. 5. Stratigraphy, pollen diagram and isotopic characteristics of core LA-D.

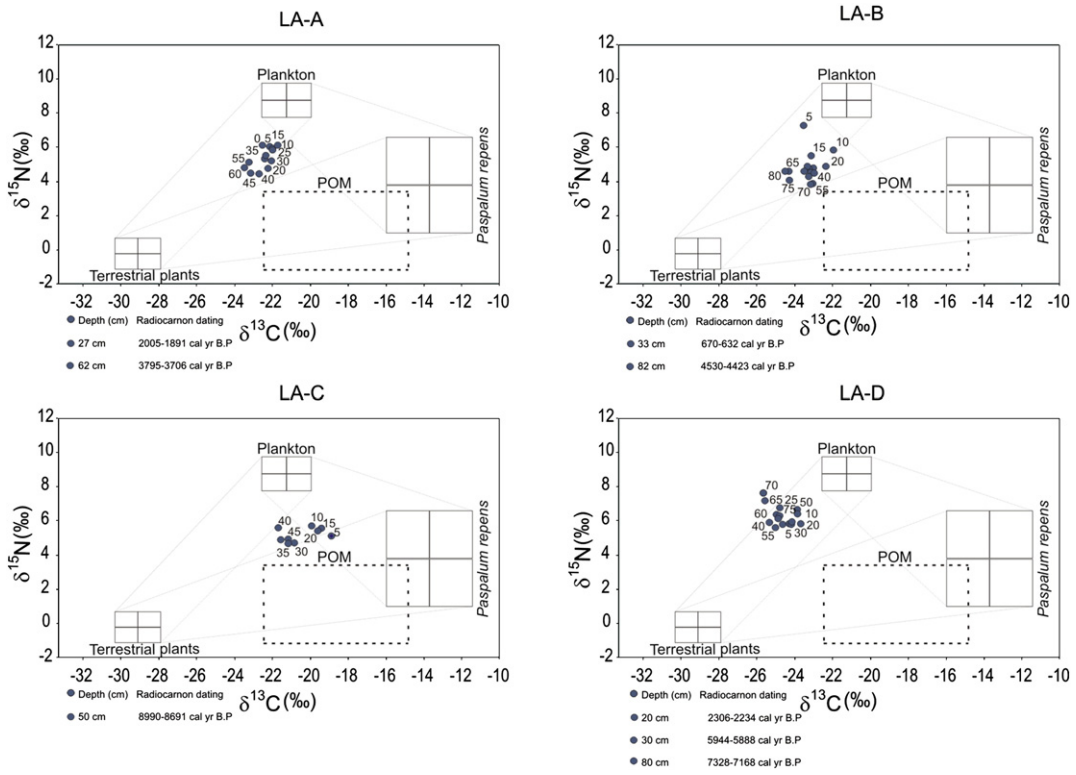

Fig. 6. Relationship between $\delta^{15}N$ and $\delta^{13}C$ values of the sediments, with interpretation according to data presented by Peterson and Howarth (1987) and Fellerhoff et al. (2003).

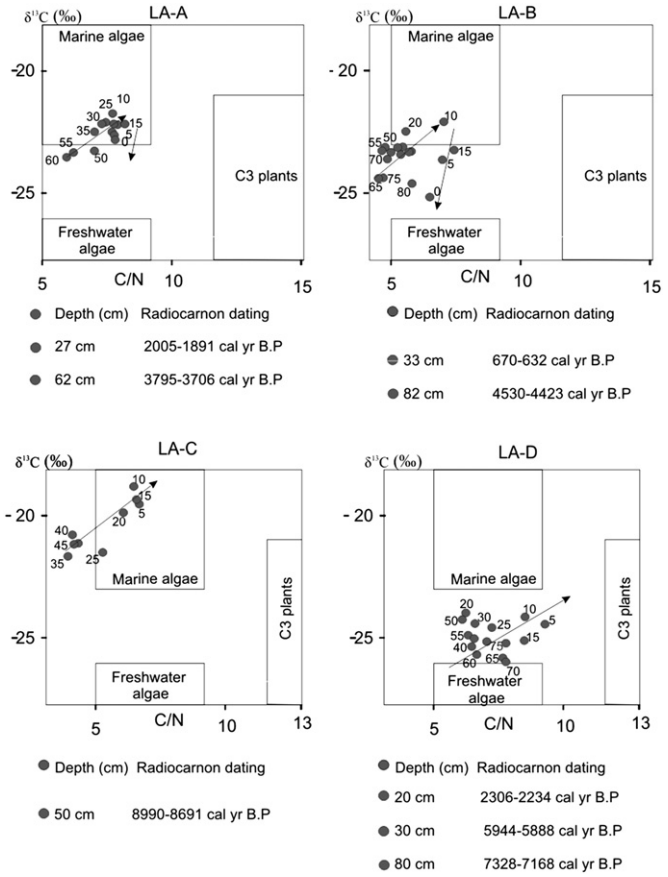

Fig. 7. Relationship between $\delta^{13}C$ and C/N values of the sediments, with interpretation according to data presented by Lamb et al. (2006); Meyers (2003) and Wilson et al. (2005a,b).

Miranda et al. (2009), based on $\delta^{13}C$, $\delta^{15}N$ and C/N data obtained 13 km away from Lake Arari, proposed a transition from aquatic to terrestrial organic matter sources during the Holocene.

5.2. Lagoon/lake transition

Between 7330–7170 and 5940–5890 cal yr B.P., the clay layers of the LA-D core (Fig. 5) indicate low flow energy with intermittent sand input during relatively higher flow energy with wave structures. During this time interval, mangroves occurred in the drainage basin of Lake Arari (Fig. 8) and the $\delta^{13}C$, $\delta^{15}N$ and C/N ratio values of sediment organic matter are in the range of typical estuarine environments (Figs. 6d and 7d), while the analysis of the LA-C core indicates organic matter derived from marine algae (Fig. 7c) during the last 8990–8690 cal yr B.P. The modern deposition of aquatic organic matter into the lake was of freshwater origin at all sampling sites.

The mangrove period ended around 2310–2230 cal yr B.P. in the LA-D core. During the last ~2200 cal yr, the LA-D core displays elemental and isotopic characteristics of terrestrial organic matter origin (Figs. 5 and 7). The pollen and stratigraphic analyses indicate significant changes in vegetation (predominance of herbs) and low sedimentation energy.

The northern sector of Lake Arari is represented by core LA-B (Fig. 1), and shows a decrease in flow energy with herbaceous and mangrove pollen between 4530–4420 and ~3000 cal yr B.P. (Fig. 3). During this time interval, the $\delta^{13}C$ and C/N values indicate contributions of marine and estuarine algae (Fig. 7b). The ~3000–670–630 cal yr B.P. interval is characterized by a decrease in flow energy and the sediments contain only herbaceous pollen (Fig. 3) with estuarine and marine algae-derived organic matter (Figs. 6b and 7b). The reduction in flow energy is characterized in the period 670–630 cal yr B.P.–modern with herbaceous pollen and an increase in organic matter originating from freshwater algae (Figs. 3 and 7b).

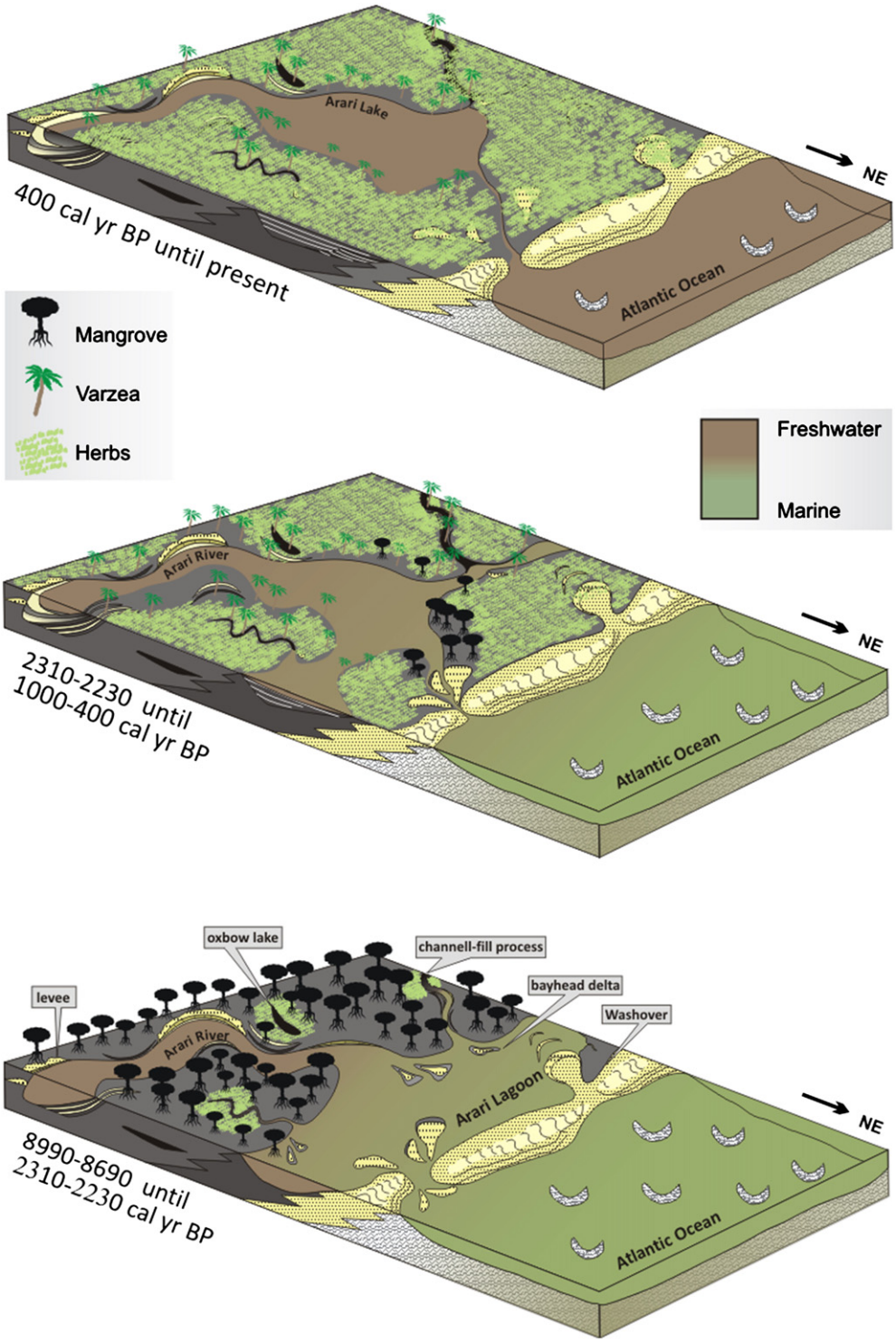

Fig. 8. Schematic representation of successive phases of sediment accumulation and vegetation change in the study area according to marine–freshwater influence gradient.

From 3790–3710 to ~2800 cal yr B.P, data for the LA-A core (Fig. 2) indicate a decreasing trend in flow energy, with the presence of herbaceous and mangrove pollen (Fig. 2) which accumulated along with organic matter predominantly of marine algal origin (Figs. 6a and 7a). From ~2800 to 2000–1890 cal yr B.P., flow energy was variable (low and relatively high), herbaceous vegetation was dominant and the organic matter is of marine algal origin (Fig. 7a). From 2000–1890 to ~800 cal yr B.P., sediments were deposited under very low flow energy with episodes of relatively higher flow energy, and preserved herbaceous pollen. A transition from marine to estuarine environments is suggested by the elemental and isotopic analyses (Fig. 7a).

The calculated sedimentation rates to the Lake Arari core are between 0.03 and 0.47 mm/yr. The cores LA-A and LA-B, sampled near the Tartatugas Channel and with higher influence of marine water, record the mid and late Holocene, and present relatively higher sedimentation rates: LA-A presents 0.2 (62–27 cm) and 0.13 mm/yr (27–0 cm), while the LA-B shows 0.13 (82–33 cm) and 0.47 mm/yr (33–0 cm). The cores LA-D and LA-C, sampled near the Arari River and on the center of the lake, record almost throughout the Holocene

and presents mainly low sedimentation rates: LA-C exhibits 0.06 mm/yr (50–0 cm), and LA-D around 0.37 mm/yr (80–30 cm), 0.03 mm/yr (30–20 cm) and 0.09 mm/yr (20–0 cm). Therefore, the cores LA-A and LA-B present higher sedimentation rates than LA-C and LA-D during the last 4500 cal yr B.P. This difference in the sedimentation rates may be related to the process of preferential filling near the connection between the old lagoon and the sea (Fig. 8).

Regarding the pollen absence between 3000 and 2000 cal yr BP in core LA-A and along the LA-C, it may be caused by various external factors (sediment grain size, microbial attack, oxidation, mechanical forces, high temperature), as well as factors inherent to the pollen grains themselves (sporopollenine content, chemical and physical composition of the pollen wall) (see Havinga, 1967). In the case of 3000–2000 cal yr BP interval in core LA-A, the sediment grain size may be considered the main cause to the absence of mangrove pollen, since during this interval occurs sandy silt layers interbedded with fine-grained sand. Sandy sediments are not suitable to the pollen preservation. However, the core LA-C presents mud sediments without pollen, it may be attributed to an eventual prolonged exposition to the atmospheric air that produces pollen oxidation (e.g. Keil et al., 1994).

Therefore, between 8990–8690 and 2310–2230 cal yr B.P., the data suggest the presence of a lagoon with strong marine influence (Fig. 8). However, during 2310–2230 and ~1000 cal yr B.P. interval, an estuarine/freshwater influence is suggested by the replacement of mangrove by herbaceous vegetation. Today, Lake Arari is dominated by freshwater with a very small tidal channel connecting the lake to the freshwaters across Marajó Island, and the phytoplankton currently found in Lake Arari is typical of freshwater (Fig. 8).

5.3. Sea-level, Amazon River discharge and climatic changes controlling wetlands dynamics

The post-glacial sea-level rise caused a marine incursion in Lake Arari at least since ~9000 cal yr B.P., and the relative sea-level along the littoral of Northern Brazil reached the modern sea-level between 7000 and 5000 cal yr B.P. (Behling, 2002; Behling and Costa, 2001; Behling et al., 2001a; Cohen et al., 2005a; Souza Filho et al., 2006, 2009; Vedel et al., 2006). The stratigraphic framework of Marajó Island, which is located in the mouth of Amazon River, shows a transgressive phase which took place in the early to mid Holocene. Subsequently, there was a shift back to more continental conditions which still prevail today in the center of Marajó Island (Rossetti et al., 2008a).

Although there was a wide connection between the old lagoon and the sea during the early and mid-Holocene (Fig. 8), the magnitude of the relative sea-level rise alone was not sufficient to produce a marine incursion into Marajó Island. This is due to the fact that, during the last 5000 years, the relative sea-level did not oscillate significantly along the coast of Northern Brazil (Cohen et al., 2005a; Souza Filho et al., 2006), and freshwater discharge from modern rivers on Marajó Island maintained low tidal water salinity (0–6‰, Santos et al., 2008). Consequently, mangroves are limited to a narrow zone on northeastern Marajó Island (Cohen et al., 2008). Thus, during the early and mid-Holocene, freshwater discharge from rivers may have been lower than today, and the post-glacial eustatic sea-level rise produced an increase in tidal water salinity.

Considering the river system as an integrator of rainfall over large areas (Amarasekera et al.;, 1997), variations in Amazon River discharge during the Holocene may be a consequence of changes in rainfall rates. Thus, the proposed relatively low fresh water discharge during the early and mid-Holocene may be a consequence of the dry periods recorded in different parts of South America. For example, the climatic conditions in the tropical Andes were significantly drier than at present between 9200 and 4400 cal yr B.P. (Moy et al., 2002; Paduano et al., 2003; Seltzer et al., 1995; Thompson et al., 1995, 2000). Baker et al. (2001) demonstrated that the maximum aridity and lowest level of Lake Titicaca occurred between 8000 and5500 cal yr B.P. In the eastern Bolivian Andes, a replacement of cloud forest by open, grass-dominated ecosystems occurred between 10,000 and 4000 yr B.P (Mourguiart and Ledru, 2003). Palaeoecological records from lakes in the Peruvian Amazon indicate a dry event from 7200 yr B.P until 3300 cal yr B.P (Bush et al., 2007). In lowland Amazonian Ecuador, periods of severe drought caused significant tree mortality between 8700 and 5800 cal yr BP, and after 5800 cal yr BP, more uniform conditions allowed the development of mature forests (Weng et al., 2002). In the Colombian Amazon, drier early Holocene and wetter late Holocene conditions are also reported (Behling and Hooghiemstra, 2000). Concomitantly, the drier period caused the replacement of forest by open savanna in the Amazon region, which in turn gave way to forest again when precipitation increased in the late Holocene (Absy et al., 1991; Bush and Colinvaux, 1988; Desjardins et al., 1996; Freitas et al., 2001; Sifeddine et al., 2001). This trend is similar to other documented forest-savanna vegetation changes in the Amazon basin during the early and middle Holocene (Behling and Costa, 2000; Gouveia et al., 1997; Sifeddine et al., 1994).

On the Maranhão littoral, eastern Amazon region, isotopic analyses of soil organic matter collected in forested and woody savanna areas indicate that from approximately 10,000 and 9000 cal yr B.P. to 4000 cal yr B.P., a woody savanna expanded, probably reflecting a drier climate (Pessenda et al., 2004a). From 4000 to 3000 cal yr B.P. to the present, there was a moderate and progressive increase in arboreal vegetation in the southern Amazon basin, due to the return to more humid climate conditions, probably similar to the present day (Freitas, et al., 2001; Pessenda et al., 2004a,b). Other isotopic studies in the southern Amazon region and on a 1600 km transect covering three states of the northeastern region, ~3000 km away from the study site, indicate a drier climate during the mid-Holocene, while the data reflect forest expansion associated to a wetter period in the last 3000 years (Pessenda et al., 1998a,b,c). Sedimentological studies in the Brazilian Amazon also indicate a wet period between 5000 and 2500 yr B.P. (Rossetti et al., 2005).

These climatic fluctuations in the Amazonian hydrographic region control the volume of the Amazon River's inflow (Haberle et al., 1999; Harris and Mix, 1999). Consequently, during the early and mid-Holocene the Amazon River's inflow was severely reduced (Maslin and Burns, 2000; Maslin et al., 2000). Irion et al. (2009) suggest that during the dry period, the sea level rise caused a backwater effect which reached far upstream, with the silting up of the Amazon valley and the inflow of the tributaries. This allowed the development of the Amazon River floodplain in its modern setting around 5000 years B.P., when the sea level reached its present level. Afterward, with the return of a more humid climate in the region, the greater discharge of the Amazon River promoted the progressive reduction of water salinity. At present, the littoral of Marajó Island is flooded by tidal freshwater (Rosario et al., 2009; Santos et al., 2008; Vinzon et al., 2008) that favors the development of freshwater vegetation and restricts mangroves to tidal flats (Cohen et al., 2008).

6. Conclusion

Physical, biological and biogeochemical data allowed the reconstruction of the depositional environment and vegetation during the Holocene. This study identified an influence between marine and freshwater with three development stages of Lake Arari: the period from 8990–8690 cal yr B.P. to 2310–2230 cal yr B.P. is characterized by strong marine influence throughout the study region represented by the wavy occurrence, mangrove colonization and accumulation of organic matter from marine algae. It is likely that during this period the connection to the sea was wider than it is today, which contributed to the development of a lagoon. Between 2310–2230 cal yr B.P. and ~1000 cal yr B.P., the mangrove was replaced by herbaceous

vegetation in agreement with the reduction of marine influence, likely due to the rise in freshwater river discharge. During the last 1000 years, Lake Arari established itself along with the expansion of herbaceous vegetation dominated by freshwater influence.

Acknowledgments

This work was funded by CNPq (Project 562398/2008-2). The first and second authors hold a scholarship from CNPq (Process 140034/2007-2 and 302943/2008-0). The authors thank student Mariah Izar Francisquini of the C-14 Laboratory of CENA-USP for her support in sediment preparation for isotope determination.

References

Absy, M.L., Cleef, A., Fournier, M., Martin, L., Servant, M., Sifeddine, A., Silva, M.F., Soubie's, F., Suguio, K., Turcq, B., Van der Hammen, T., 1991. Mise en évidence de quatre phases d'ouverture de la forêt dense dans le sud-est de l'Amazonie au cours des 60,000 dernières années. Première comparaison avec d'autres régions tropicales. Comptes Rendus de l'Academie des Sciences de Paris 312 (II), 673–678.

Amarasekera, K.N., Lee, R.F., Williams, E.R., Eltahir, E.A.B., 1997. ENSO and the natural variability in the flow of tropical rivers. Journal of Hydrology 200, 24–39.

Baker, P.A., Seltzer, G.O., Fritz, S.C., Dunbar, R.B., Grove, M.J., Tapia, P.M., Cross, S.L., Rowe, H.D., Broda, J.P., 2001. The history of South American tropical precipitation for the past 25,000 years. Science 291, 640–643.

Behling, H., 2002. Carbon storage increases by major forest ecosystems in tropical South America since the Last Glacial Maximum and the early Holocene. Global and Planetary Change 33, 107–116.

Behling, H., Costa, M.L., 2000. Holocene environmental changes from the Rio Curuá record in the Caxiuanã region, eastern Amazon Basin. Quaternary Research 53, 369–377.

Behling, H., Costa, M.L., 2001. Holocene vegetational and coastal environmental changes from the Lago Crispim record in northeastern Pará State, eastern Amazonia. Review of Palaeobotany and Palynology 114, 145–155.

Behling, H., Hooghiemstra, H., 2000. Holocene Amazon rainforest–savanna dynamics and climatic implications: high-resolution pollen record from Laguna Loma Linda in eastern Colombia. Journal of Quaternary Science 15, 687–695.

Behling, H., Cohen, M.C.L., Lara, R.J., 2001a. Studies on Holocene mangrove ecosystem dynamics of the Bragança Peninsula in north-eastern Pará, Brazil. Palaeogeography, Palaeoclimatology, Palaeoecology 167, 225–242.

Behling, H., Keim, G., Irion, G., Junk, W., Mello, J.N., 2001b. Holocene environmental-changes in the Central Amazon Basin inferred from Lago Calado (Brazil). Palaeogeography, Palaeoclimatology, Palaeoecology 173, 87–101.

Behling, H., Cohen, M.C.L., Lara, R.J., 2004. Late Holocene mangrove dynamics of the Marajó Island in northern Brazil. Vegetation History and Archaeobotany 13, 73–80.

Bicudo, C.E.M., 1970. Algas de águas continentais brasileiras: chave ilustrada para identificação dos gêneros. EDUSP, São Paulo, pp. 1–228.

Blasco, F., Saenger, P., Janodet, E., 1996. Mangroves as indicators of coastal change. Catena 27, 167–178.

Boggs, S., 2012. Principles of Sedimentology and Stratigraphy. Prentice Hall, New Jersey, p. 600.

Bourrelly, P., 1972. Les algues d'eau douce: Initiation à la systématique. Les algues vertes, Tome I. Éditions M. Boubée & Cie. (Collection "Faunes et Flore Actuelly"), Paris, pp. 1–509.

Bush, M.B., Colinvaux, P.A., 1988. A 7000-year pollen record from the Amazon lowlands, Ecuador. Vegetatio 76, 141–154.

Bush, M.B., Silman, M.R., Listopad, C.M.C.S., 2007. A regional study of Holocene climate change and human occupation in Peruvian Amazonia. Journal of Biogeography 34, 1342–1356.

Camargo, M.G., 1999. SYSGRAN for Windows: Granulometric Analyses System. Pontal do Sul. Paraná, Brasil.

Cleve-Euler, A., 1953. Die Diatomeen von Schweeden und Finland. Bihang K. Svenska Vetenskapsakademiens Handlingar, 2, pp. 1–163.

Cohen, M.C.L., Behling, H., Lara, R.J., 2005a. Amazonian mangrove dynamics during the Last Millennium: the relative sea-level and the Little Ice Age. Review of Palaeobotany and Palynology 136, 93–108.

Cohen, M.C.L., Souza Filho, P.W., Lara, R.L., Behling, H., Angulo, R., 2005b. A model of Holocene mangrove development and relative sea-level changes on the Bragança Peninsula (northern Brazil). Wetland Ecology and Management 13, 433–443.

Cohen, M.C.L., Lara, R.J., Smith, C.B., Angelica, R.S., Dias, B.S., Pequeno, T., 2008. Wetland dynamics of Marajó Island, northern Brazil during the last 1000 years. Catena 76, 70–77.

Cohen, M.C.L., Behling, H., Lara, R.J., Smith, C.B., Matos, H.R.S., Vedel, V., 2009. Impact of sea-level and climatic changes on the Amazon coastal wetlands during the late Holocene. Vegetation History and Archaeobotany 18, 1–15.

Colinvaux, P.A., De Oliveira, P.E., Patiño, J.E.M., 1999. Amazon Pollen Manual and Atlas. Hardwood, Amsterdam, p. 332.

Cooper, S.R., 1999. Estuarine paleoenvironmental reconstructions using diatoms. In: Stoermer, E.F., Smol, J.P. (Eds.), The Diatoms: Applications for the Environmental and Sciences. University Press, Cambridge, pp. 352–373.

Desikachary, T.S., 1959. Cyanophyta. Concil of Agricultura Researcer, Indian, pp. 1–686.

Desjardins, T., Filho, A.C., Mariotto, A., Chauvel, A., Girardin, C., 1996. Changes of the Forest-savannah boundary in Brazilian Amazonia during the Holocene as revealed by soil organic carbon isotope ratios. Oecologia 108, 749–756.

Faegri, K., Iversen, J., 1989. Textbook of Pollen AnalysisIV Edition. J. Wiley & Sons, New York.

Fellerhoff, C., Voss, M., Wantzen, K.M., 2003. Stable carbon and nitrogen isotope signatures of decomposing tropical macrophytes. Aquatic Ecology 37, 361–375.

Förster, V.K., 1974. Amazonische demidieen. Amazoniana, Manaus, pp. 135–242.

Freitas, H.A., Pessenda, L.C.R., Aravena, R., Gouveia, S.E.M., Ribeiro, A.S., Boulet, R., 2001. Late Quaternary climate change in southern Amazon inferred from 17,000 years vegetation dynamic record from soil organic matter, using $\delta^{13}C$ and ^{14}C dating. Quaternary Research 55, 39–46.

Gouveia, S.E.M., Pessenda, L.C.R., Aravena, R., Boulet, R., Roveratti, R., Gomes, B.M., 1997. Dinâmica de vegetações durante o Quaternário recente no sul do Amazonas indicada pelos isótopos do carbono (12C, 13C e 14C). Geochimica Brasiliensis 11, 355–367.

Gouveia, S.E.M., Pessenda, L.C.R., Aravena, R., 1999. Datação da fração humina da matéria orgânica do solo e sua comparação com idades 14C de carvões fósseis. Química Nova 22, 810–814.

Grimm, E.C., 1987. CONISS: a Fortran 77 program for stratigraphically constrained cluster analysis by the method of the incremental sum of squares. Pergamon Journals 13, 13–35.

Guimarães, J.T.F., Cohen, M.C.L., França, M.C., Lara, R.J., Behling, H., 2010. Model of wetland development of the Amapá littoral during the Late Holocene. Anais da Academia Brasileira de Ciências 82, 1–15.

Haberle, S.G., Mark, A., Maslin, M.A., 1999. Late Quaternary vegetation and climate change in the Amazon Basin based on a 50,000 year pollen record from the Amazon Fan, ODP Site 932. Quaternary Research 51, 27–38.

Harris, S.E., Mix, A.C., 1999. Pleistocene precipitation balance in the Amazon Basin recorded in deep sea sediments. Quaternary Research 51, 14–26.

Havinga, A.J., 1967. Palynology and pollen preservation. Review of Palaeobotany and Palynology 2, 81–98.

Herrera, L.F., Urrego, L.E., 1996. Atlas de polen de plantas útiles y cultivadas de la Amazonia colombiana (Pollen atlas of useful and cultivated plants in the Colombian Amazon region). Estudios en la Amazonia Colombiana XI. Tropenbos-Colombia, Bogotá, p. 462.

Hino, K., Tundisi, J., 1984. Atlas de algas da Represa do Broa. Universidade Federal de São Carlos, São Carlos, pp. 1–143.

Hustedt, F., 1930. Die Kieselalgen. Deutschlands, Osterreichs und der Schweiz. In: RABENHOST, L. (Ed.), Kryptogamen-flora von Deutschlands, Osterreich und der Schweiz. Akademische Verlagsgesellschaft, Portigh, pp. 1–920.

IDESP, 1974. Institute of social and economic development of the Pará. Integrated studies of Marajó Island, p. 333. Belém.

Irion, G., Müller, J., Morais, J.O., Keim, G., Nunes de Mello, J., Junk, W.J., 2009. The impact of Quaternary sea level changes on the evolution of the Amazonian lowland. Hydrological Processes 23, 3168–3172.

Keil, R.G., Hu, F.S., Tsamakis, E.C., Hedges, J.I., 1994. Pollen in marine sediments as indicator of oxidation of organic matter. Nature 369, 639–641.

Komárek, J., Fott, B., 1983. Chlorophyceae (Grünalgen). Chlorococcales. In: Huber-Pestalozzi, G. (Ed.), Das phytoplankton des süssawassers: systematic und biologie, 7(1). E. Scweizerbart'sche Verlagsbuchlandlung, Stuttgart.

Krauss, K.W., Lovelock, C.E., McKee, K.L., López-Hoffman, L., Ewe, S.M.L., Sousa, W.P., 2008. Environmental drivers in mangrove establishment and early development: a review. Aquatic Botany 89, 105–127.

Lamb, A.L., Wilson, G.P., Leng, M.J., 2006. A review of coastal palaeoclimate and relative sea-level reconstructions using δ13C and C/N ratios in organic material. Earth-Science Reviews 75, 29–57.

Lara, R.J., Cohen, M.C.L., 2009. Palaeolimnological studies and ancient maps confirm secular climate fluctuations in Amazonia. Climatic Change 94, 399–408.

Lima, C.M., 2008. Dinâmica da vegetação e inferências climáticas no Quaternário Tardio na região da Ilha de Marajó (PA), empregando os isótopos do carbono (12C,13C,14C) da matéria orgânica de solos e sedimentos. Dissertação (Mestrado em Ciências)- Centro de Energia Nuclear na Agricultura da Universidade de São Paulo. p. 182.

Maslin, M.A., Burns, S.J., 2000. Reconstruction of the Amazon Basin effective moisture availability over the past 14,000 years. Science 290, 2285–2287.

Maslin, M.A., Durham, E., Burns, S.J., Platzman, E., Grootes, P., Greig, S.E.J., Nadeau, M.-J., Schleicher, M., Pflaumann, U., Lomax, B., Rimington, N., 2000. Palaeoreconstruction of the Amazon River freshwater and sediment discharge using sediments recovered at Site 942 on the Amazon Fan. Journal of Quaternary Science 15, 419–434.

Meyers, P.A., 1994. Preservation of elemental and isotopic source identification of sedimentary organic matter. Chemical Geology 144, 289–302.

Meyers, P.A., 2003. Applications of organic geochemistry to paleolimnological reconstructions: a summary of examples from the Laurentian Great Lakes. Organic Geochemistry 34, 261–289.

Meyers, P.A., Lallier-Vergès, E., 1999. Lacustrine sedimentary organic matter records of Late Quaternary paleoclimates. Journal of Paleolimnology 21, 345–372.

Miranda, M.C.C., Rossetti, D.F., Luiz Carlos Ruiz Pessenda, L.C.R., 2009. Quaternary paleoenvironments and relative sea-level changes in Marajó Island (Northern Brazil): Facies, δ13C, δ15N and C/N. Palaeogeography, Palaeoclimatology, Palaeoecology 282, 19–31.

Monteiro, M.D.R., Melo, N.F.A.C., Alves, M.A.M., da, S., Paiva, R.S., 2009. Composição e distribuição do microfitoplâncton do rio Guamá no trecho entre Belém e São Miguel do Guamá, Pará, Brasil. Boletim do Museu Paraense Emílio Goeldi. Ciências Naturais 4, 341–351.

Moreira, L.S., Moreira-Turcq, P.F., Cordeiro, R.C., Turcq, B.J., 2009. Reconstituição paleoambiental do Lago Santa Ninha, Várzea do Lago Grande de Curuai, Pará, Brasil. Acta Amazonica 39, 609–616.

Moreira-Turcq, P., Jouanneau, J.M., Turcq, B., Seyler, P., Weber, O., Guyot, J.L., 2004. Carbon sedimentation at Lago Grande de Curuai, a floodplain lake in the low Amazon region: insights into sedimentation rates. Palaeogeography, Palaeoclimatology, Palaeoecology 214, 27–40.

Mourguiart, P., Ledru, M.P., 2003. Last Glacial Maximum in an Andean cloud forest environment (Eastern Cordillera, Bolivia). Geology 31, 195–198.

Moy, C.M., Seltzer, G.O., Rodbell, D.T., Anderson, D.M., 2002. Variability of El Nino/Southern Oscillation activity at millennial timescales during the Holocene epoch. Nature 420, 162–165.

Navarro, J.N., Peribonio, R.G., 1993. A light and scanning electron microscope study of the centric diatom *Polymyxus coronalis* (Bacillariophyta). European Journal of Phycology 28, 167–172.

Paduano, G.M., Bush, M.B., Baker, P.A., Fritz, S.C., Seltzer, G.O., 2003. A vegetation and fire history of Lake Titicaca since the Last Glacial Maximum. Palaeogeography, Palaeoclimatology, Palaeoecology 194, 259–279.

Paiva, R.S., Esquinaze-Leça, E., Passavante, J.Z.O., Silva-Cunha, M.G.G., Melo, N.F.A.C., 2006. Considerações ecológicas sobre o fitoplâncton da baía do Guajará e foz do rio Guamá (Pará-Brasil). Boletim do Museu Paraense Emílio Goeldi. Ciências Naturais 1, 133–146.

Parra, O.O., Bicudo, C.E.M., 1995. Introduccion a la Sistematica de Las Algas de Aguas Continentales. Gráfica Andes Ltda, Santiago.

Peragallo, H., Peragallo, M., 1897–1908. Diatomees marines de France et des districts maritimes voisins. M. J. Tempère, Paris, pp. 1–492.

Pessenda, L.C.R., Aravena, R., Melfi, A.J., Boulet, R., 1996. The use ofcarbon isotopes (13C, 14C) in soil to evaluate vegetation changes during the Holocene in central Brazil. Radiocarbon 38, 191–201.

Pessenda, L.C.R., Gouveia, S.E.M., Aravena, R., Gomes, B.M., Boulet, R., Ribeiro, A.S., 1998a. ^{14}C dating and stable carbon isotopes of soil organic matter in forest-savanna boundary areas in the southern Brazilian Amazon region. In: Wasserman, J.C., Silva-Filho, E., Villas-Boas, R. (Eds.), Environmental Geochemistry in the Tropics. Springer-Verlag, Berlin, pp. 7–16.

Pessenda, L.C.R., Gomes, B.M., Aravena, R., Ribeiro, A.S., Boulet, R., Gouveia, S.E.M., 1998b. The carbon isotope record in soils along a forest-cerrado ecosystem transect: implications for vegetation changes in the Rondonia state, southwestern Brazilian Amazon region. The Holocene 8, 631–635.

Pessenda, L.C.R., Gouveia, S.E.M., Aravena, R., Gomes, B.M., Boulet, R., Ribeiro, A.S., 1998c. 14C dating and stable carbon isotopes of soil organic matter in forest-savanna boundary areas in the southern Brazilian Amazon region. Radiocarbon 40, 1013–1022.

Pessenda, L.C.R., Boulet, R., Aravena, R., Rosolen, V., Gouveia, S.E.M., Ribeiro, A.S., Lamotte, M., 2001a. Origin and dynamics of soil organic matter and vegetation changes during the Holocene in a forest–savanna transition zone, Brazilian Amazon region. The Holocene 11, 250–254.

Pessenda, L.C.R., Gouveia, S.E.M., Aravena, R., 2001b. Radiocarbon dating of total soil organic matter and humin fraction, and comparison with 14C ages of fossil charcoal. Radiocarbon 43, 595–601.

Pessenda, L.C.R., Ribeiro, A.S., Gouveia, S.E.M., Aravena, R., Boulet, R., Bendassoli, J.A., 2004a. Vegetation dynamics during the late Pleistocene in the Barreirinhas region, Maranhão State, northeastern Brazil, based on carbon isotopes in soil organic matter. Quaternary Research 62, 183–193.

Pessenda, L.C.R., Gouveia, S.E.M., Aravena, R., Boulet, R., Valencia, E.P.E., 2004b. Holocene fire and vegetation changes in southeastern Brazil as deduced from fossil charcoal and soil carbon isotopes. Quaternary International 114, 35–43.

Pessenda, L.C.R., Gouveia, S.E.M., Ribeiro, A.S., De Oliveira, P.E., Aravena, R., 2010. Late Pleistocene and Holocene vegetation changes in the northeastern Brazil determinedfrom carbon isotopes and charcoal records in soils. Palaeogeography, Palaeoclimatology, Palaeoecology 297, 507–608.

Peterson, B.J., Howarth, R.W., 1987. Sulfur, carbon, and nitrogen isotopes used to trace organic matter flow in the salt-marsh estuary of Sapelo Island, Georgia. Limnology and Oceanography 32, 1195–1213.

Reimer, P.J., Baillie, M.G.L., Bard, E., Bayliss, A., Beck, J.W., Bertrand, C.J.H., Blackwell, P.G., Buck, C.E., Burr, G.S., Cutler, K.B., Damon, P.E., Edwards, R.L., Fairbanks, R.G., Friedrich, M., Guilderson, T.P., Hogg, A.G., Hughen, K.A., Kromer, B., McCormac, F.G., Manning, S.W., Ramsey, C.B., Reimer, R.W., Remmele, S., Southon, J.R., Stuiver, M., Talamo, S., Taylor, F.W., Van der Plicht, J., Weyhenmeyer, C.E., 2004. IntCal04 Terrestrial radiocarbon age calibration, 26–0 ka BP. Radiocarbon 46, 1029–1058.

Rosario, R.P., Bezerra, M.O.M., Vinzon, S.B., 2009. Dynamics of the saline front in the Northen Channel of the Amazon River — influence of fluvial flow and tidal range (Brazil). Journal of Coastal Research 2, 503–514.

Rossetti, D.F., Toledo, P.M., Góes, A.M., 2005. New geological framework for the Western Amazonia: implications for biogeography and evolution. Quaternary Research 63, 78–89.

Rossetti, D.F., Valeriano, M.M., Góes, A.M., Thalles, M., 2008a. Palaeodrainage on Marajó Island, northern Brazil, in relation to Holocene relative sea-level dynamics. The Holocece 18, 1–12.

Rossetti, D.F., Góes, A.M., Valeriano, M.M., Miranda, M.C., 2008b. Quaternary tectonics in a passive margin: Marajó Island, northern Brazil. Journal of Quaternary Science 23, 121–135.

Rossetti, D.F., Almeida, S., Amaral, D.D., Lima, C.M., Pessenda, L.C.R., 2010. Coexistence of forest and savanna in an Amazonian area from a geological perspective. Journal of Vegetation Science 21, 120–132.

Roubik, D.W., Moreno, J.E., 1991. Pollen and Spores of Barro Colorado Island, vol. 36. Missouri Botanical Garden, St. Louis, p. 268.

Round, F.E., Crawford, R.M., Mann, D.G., 1990. The Diatoms: Biology and Morphology of the Genera. Cambridge University Press, Cambridge, pp. 1–747.

Santos, M.L.S., Medeiros, C., Muniz, K., Feitosa, F.A.N., Schwamborn, R., Macedo, S.J., 2008. Influence of the Amazon and Pará rivers on water composition and phytoplankton biomass on the adjacent shelf. Journal of Coastal Research 24, 585–593.

Seltzer, G.O., Rodbell, D.T., Abbott, M., 1995. Andean glacial lakes and climate variability since the Last Glacial Maximum. Bulletin - Institut Francais d'Etudes Andines 24, 539–549.

Sharp, Z., 2007. Principles of Stable Isotope Geochemistry. Pearson Prentice Hall, UpperSaddle Ridge, New Jersey.

Sifeddine, A., Fröhlich, F., Fournier, M., Martin, L., Servant, M., Soubiès, F., Turcq, B., Suguio, K., Volkmer-Ribeiro, C., 1994. La sedimentation lacustre indicateur de changements des paléoenvironnements au cous des 30.000 dernières années (Carajás, Amazonie, Brésil). Géociences de surface 1645–1652.

Sifeddine, A., Martin, L., Turcq, B., Volkmer-Ribeiro, C., Soubies, F., Cordeiro, R.C., Suguio, K., 2001. Variations of the Amazonian rainforest environment: a sedimentological record covering 30,000 years. Palaeogeography, Palaeoclimatology, Palaeoecology 168, 221–235.

Souza Filho, P.W.M., Cohen, M.C.L., Lara, R.J., Lessa, G.C., Koch, B., Behling, H., 2006. Holocene coastal evolution and facies model of the Bragança macrotidal flat on the Amazon Mangrove Coast, Northern Brazil. Journal of Coastal Research 39, 306–310.

Souza Filho, P.W.M., Lessa, G.C., Cohen, M.C.L., Costa, F.R., Lara, R.J., 2009. The subsiding macrotidal barrier estuarine system of the Eastern Amazon Coast, Northern Brazil, In: Dilleburg, S.F., Hesp, P.A. (Eds.), Geology and Geomophology of Holocene Coastal Barriens of Brazil, 1 ed. Springer, New York, pp. 347–375.

Thompson, L.G., Mosley-Thompson, E., Davis, M.E., Lin, P.-N., Henderson, K.A., Cole-Dai, J., Bolsan, J.F., Liu, K.G., 1995. Late glacial stage and Holocene tropical ice core records from Huascaran, Peru. Science 269, 46–50.

Thompson, L.G., Mosley-Thompson, E., Henderson, K.A., 2000. Ice core palaeoclimate records in tropical South America since the Last Glacial Maximum. Journal of Quaternary Science 15, 377–394.

Toledo, M.B., Bush, M.B., 2007. A mid-Holocene environmental change in Amazonian savannas. Journal of Biogeography 34, 1313–1326.

Troxler, T.G., Richards, J.H., 2009. δ13C, δ15N, carbon, nitrogen and phosphorus as indicators of plant ecophysiology and organic matter pathways in Everglads deep slough, Florida, USA. Aquatic Botany 91, 157–165.

Turcq, B., Albuquerque, A.L.S., Cordeiro, R.C., Sifeddine, A., Simoes Filho, F.F.L., Souza, A.G., Abrão, J.J., Oliveira, F.B.L., Silva, A.O., Capitâneo, J., 2002. Accumulation of organic carbon in five Brazilian lakes during the Holocene. Sedimentary Geology 148, 319–342.

Vedel, V., Behling, H., Cohen, M.C.L., Lara, R.J., 2006. Holocene mangrove dynamics and sea-level changes in northern Brazil, inferences from the Taperebal core in northeastern Pará State. Vegetation History and Archaeobotany 15, 115–123.

Vinzon, B.S., Vilela, C.P.X., Pereira, L.C.C., 2008. Processos físicos na Plataforma Continental Amazônica. Relatório-Técnico, Potenciais Impactos Ambientais do Transporte de Petróleo e Derivados na Zona Costeira Amazônico. Petrobrás, Brasil, p. 31.

Weng, C., Bush, M.B., Athens, J.S., 2002. Two histories of climate change and hydrarch succession in Ecuadorian Amazonia. Review of Palynology and Paleobotany 120, 73–90.

Whitmore, T.C., 2009. An Introduction to Tropical Rain Forests. Oxford University Press, New York, p. 251.

Wilson, G.P., Lamb, A.L., Leng, M.J., Gonzalez, S., Huddart, D., 2005a. Variability of organic δ13C and C/N in the Mersey Estuary, U.K. and its implications for sea-level reconstruction studies. Estuarine, Coastal and Shelf Science 64, 685–698.

Wilson, G.P., Lamb, A.L., Leng, M.J., Gonzalez, S., Huddart, D., 2005b. δ13C and C/N as potential coastal palaeoenvironmental indicators in the Mersey Estuary, UK. Quaternary Science Reviews 24, 2015–2029.

Woodroffe, C.D., 1982. Geomorphology and development of mangrove swamps, Grand Cayman Island, West Indies. Bulletin of Marine Science 32 (2), 381–398.